

Submitted to: Proceedings of the Health Physics Society 2008 Professional Development School - Topics in Accelerator Health Physics (Oakland CA, January 2008)

Radiation Shielding at High-Energy Electron and Proton Accelerators

Sayed H. Rokni¹, J. Donald Cossairt², James C. Liu¹

Introduction

The goal of accelerator shielding design is to protect the workers, general public, and the environment against unnecessary prompt radiation from accelerator operations. Additionally, shielding at accelerators may also be used to reduce the unwanted background in experimental detectors, to protect equipment against radiation damage, and to protect workers from potential exposure to the induced radioactivity in the machine components. The shielding design for prompt radiation hazards is the main subject of this chapter.

General Considerations in the Shielding of Accelerators

High-energy accelerators are capable of producing radiation fields of high energy and high intensity, mixed with photons and neutrons. Protection against these radiation fields can be effectively achieved by attenuating the radiation to acceptable levels with appropriate thickness and proper types of shield materials, which can be placed either locally or as structure housing.

In addition to the shielding itself, the degree to which the radiation level must be attenuated depends on several factors, such as: 1) the radiation source terms, 2) the distance from the radiation source to the dose point of interest, 3) the conservative estimate of the time that the workers or public may spend at the dose point (or the irradiation time for the object to be protected), and 4) the required dose limits outside the shield.

¹Stanford Linear Accelerator Center (SLAC), Stanford, CA, 94205

²Fermi National Accelerator Laboratory, Batavia, IL 60510

The radiation source terms and the applicable dose limits (derived from regulations and/or facility's administrative limits) provide starting points for determining shielding requirements. The radiation source terms depend on accelerator beam parameters (the type of beam particle and its energy and intensity) and accelerator operation modes, which in general are provided by accelerator or facility physicists. Various modes of accelerator operation (e.g., normal beam losses and abnormal beam losses under credible scenarios), as well as appropriate dose limits for different scenarios, need to be carefully considered in the shield design process.

In general, normal beam losses occur at specific beamline locations, such as beam absorbers or “dump” (or beam stop), collimators, beam scrapers, or other beam-defining apertures, while abnormal beam losses are assumed to occur at any point, except for locations that can specifically excluded by design. The normal-beam-loss points can then be locally shielded and the rest of the machine can be more lightly shielded. Detailed knowledge and close control of the beam operation modes and locations of beam losses, as well as alignment of these critical beam-defining devices, are necessary to ensure these important estimation and assumption used in shielding design. Exclusion of beam losses at specific locations by engineered design should verified by independent review by qualified experts and by measurement, if the latter is feasible.

Since accelerator's maximum capability may exceed its desired operating level (in energy or intensity) any potential facility upgrade should also be considered at the time of initial design to avoid the burden of major shielding modification or operation limitation in the future.

Consideration of cost and/or space could prohibit shielding for full capability of an accelerator, or for full beam losses at all locations. Therefore, in most large accelerators, a balanced combination of passive system (shielding and fence) and active systems (limiters and

detectors) can offer a cost-effective solution to meet both the safety and operational requirements. For example, active current monitors can be used to monitor and limit the beam current that is allowed to enter a beamline. Radiation monitors could also be placed inside and/or outside of the shielding wall to detect and terminate unexpected, high radiation levels. In general, the use of passive systems is preferred as the use of active systems may not provide the inherent reliability of adequate shields. The use of active system to complement the passive systems must be carefully analyzed to see if the proper degree of safety will be achieved. A complete discussion of use of active systems to augment shielding is provided in Liu, et al. (2007).

In summary, accelerator shielding design should consider the followings:

- The parameters to be considered include the maximum beam energy and intensity, average beam power, normal and abnormal beam losses, schedule and modes of operations, area classification and area occupancy.
- Shielding should be designed for maximum normal operation with allowance for occasional high beam losses.
- The maximum capability of the accelerator should be considered for targets and dumps.
- In addition to an annual dose limit for normal beam losses, a maximum dose rate limit should be established for high, but occasional, beam losses. Dose limits for radiation workers and the members of public should be considered.
- Environmental radiological impact from beam operations (activation of air, soil and groundwater) should be considered.
- The shielding design should be an integral part of the overall safety design of the accelerator.

The following checklist is recommended by Schopper et al. (1990) in arriving at a shielding specification:

- Assess the physical lay-out
- Subdivide the facility according to functional and constructional requirements
- Define the primary and secondary radiation sources and the source strengths for normal permanent operation, occasional special operations and unwanted excursions.
- Specify an overall safety factor in the source definition which must include possible future use and operations.
- Define the maximum dose/year and the maximum dose rates in areas outside the projected shielding.
- Specify the attenuation needed for all sources and areas.
- Estimate the shielding
- Define a tentative shielding layout.
- Assess the overall attenuation obtained and check for conflicting interests before proceeding with the design of the final layout.

Monte Carlo codes, such as FLUKA (Fasso 2005), MARS15 (Mokhov 1995), EGS4 (Nelson et al. 1985), MCNPX (McKinney 2007), or PHITS (Iwase 2002) provide the most accurate results for shielding design, in particular for complicated three-dimensional geometries. However, much time and effort can be saved by use of analytic methods that are widely used for solution of practical shielding problems.

In the next two sections of this chapter, the radiation source terms in high-energy electron and proton accelerators and their shielding by common shielding materials such as lead, concrete

and polyethylene using analytical and semi-empirical methods are described for high-energy electron and proton accelerators (defined as accelerators with beam energy more than 10 MeV). The underlying physical process for radiation source terms and common methods and tools for calculating shielding requirements are discussed.

Shielding of Electron Accelerators

For a high-energy electron accelerator, the underlying process involved in the production of the various prompt radiation fields is the electromagnetic (EM) cascade shower that is developed in the interactions of high energy electrons with matter, beam device or target. Only a small fraction of the energy is dissipated as a result of collision processes, such as ionization and excitation, while a large fraction is spent in the production of high energy photons (bremsstrahlung). The secondary photons, in turn, undergo materialization into electron positron pairs or make Compton collisions. These process results in the electrons having energies comparable to the photons, and the process continues until more and more electrons fall into the energy range where radiation losses no longer can compete with collision losses. Eventually the energy of the initiating particle is completely dissipated in excitation and ionization of atoms.

The electron energy at which the average energy loss due to radiation and due to ionization are equal is know as Critical Energy, E_C . The value of E_C in MeV is approximately given by

$$E_C = \frac{800}{Z + 1.2} \quad (1)$$

where Z is the atomic number of the target materials (Rossi, 1952). For electron energies above E_C , radiation losses become increasing dominant. The approximate scale length that describes the high-energy propagation of EM cascade is called, the radiation length, X_0 . It is the

mean thickness of materials over which the energy of an electron is reduced by a factor of e . At energies higher than E_c (where ionization may be neglected) the energy E of an electron at depth X is given by

$$E = E_0 e^{-X/X_0} \quad (2)$$

The radial shower distribution is usually described in terms of Molière radius X_m :

$$X_m = \frac{X_0 E_s}{E_c} \quad (3)$$

where $E_s = 21.2$ MeV

A more detailed discussion of source components of the prompt radiation fields is given in (Vylet 2007; Vylet et al. 2001). The following conclusions generally apply to high-energy electron accelerators:

- Photons and giant resonance neutrons (GRN) dominate the radiation field inside shielding enclosures and remain a significant component behind moderate shielding (e.g., less than 3-4 feet thick concrete). For example, a 60-cm-lateral concrete shielding of a 3 GeV electron beam line with average beam power of 5 watts can be considered as moderate.
- High-energy neutrons (> 100 MeV) generated in the target, and associated evaporation neutrons and photons generated in the shield, are the determining factor for design of thick shielding (e.g. thicker than 3-4 feet of concrete). In this case, the “equilibrium” neutron spectrum, in which the neutron spectral shape does not change and only the fluence is reducing as the shield becomes thicker, also exists.

- To attenuate neutrons with energies above 20 MeV, the best shielding configuration consists of a layer of high-Z (high atomic number) material, such as lead or steel, followed by a low-Z shield with high hydrogen content – most often concrete. This scheme takes advantage of high inelastic cross sections such as (n, xn) or (n, n') in high-Z materials to reduce the neutron energy effectively. The lower energy neutrons generated in this process are then best attenuated by moderation and absorption down to thermal energies in hydrogenous material. The first high-Z layer is also efficient for shielding photons of all energies.
- It is best to design beam lines so that EM showers from beam losses are fully contained in potential targets or additional local collimators or shielding, so that no further shower development can occur in concrete shielding walls. Due the distance factor and large physical size of a shower in concrete (which has a long radiation length, X_0), it could result in extremely high radiation levels outside shielding, if the shower occurs in the concrete wall.
- At energies above a few GeV, additional shielding (preferably high-Z materials) in the forward direction behind a beam loss target (such as beam dump) may be required for highly penetrating muon radiation. At very high energies completely ranging out muons using a very thick shielding may not be practical. Muon dose rates is best to be reduced by using a combination of shielding (which provides fluence attenuation by ranging out muons and multiple scattering) and taking advantage of distance, supplemented with possible use of a narrow exclusion zone around the 0° (forward) direction.

It is appropriate to review some simple shielding calculation codes useful to practitioners specifically at high-energy electron facilities. These codes make use of semi-empirical models for radiation source terms as a function of angle and attenuation lengths through matter. Such models, represented by analytical formulae and values of relevant parameters, are available in the literature and commonly written in a user-friendly code or formalism, making their utilization easier and more efficient for many (but not all) shielding problems than would be the case for detailed calculation using a state-of-the-art Monte Carlo code.

The SHIELD11 code (Nelson and Jenkins 2005) is a semi-empirical shielding code designed specifically for use at high-energy electron facilities. It was developed by Nelson and Jenkins at the Stanford Linear Accelerator Center and has been used widely in shielding of electron accelerators (Ipe and Liu 1992; Liu 1999; Liu 2001b; Rokni 1996). Its method is analogous to the Moyer model initially developed for proton machines. As shown in Fig. 1, SHIELD11 assumes a very simple geometry: a shielding slab of thickness d is located at a perpendicular distance a and at an angle α with respect to a cylindrical target of radius r and length t , which is struck by an electron beam with an energy E . The photon and neutron dose equivalent at the dose point behind the shield at various angle θ relative to beam can be calculated. Additional “local” shielding of different material, in parallel with slab shield and situated between the target and the slab shield, can also be taken into account.

Source terms for secondary radiation species generated in the target and their attenuation in the target itself and the shield are calculated using relatively simple analytical formulas derived from fits to experimental data and Monte Carlo calculations. Note that the model is based on a “thick target” assumption, requiring that the EM shower be fully developed in the target. This implies that the radius should be greater than 1 Moliere unit and the length should be

longer than 10 radiation lengths in a given material. Additional consideration for target size is needed when accounting for neutron attenuation in the target is desired. Further restrictions on radius and length are imposed in terms of relaxation length for the direct-gamma component GamD (see below).

The source terms in SHIELD11 are expressed in terms of dose equivalent rate [Sv h^{-1}] at one meter from target per kW of beam power. Only production of secondary photons and neutrons is taken into account, i.e., muons are not considered. The source terms consist of the following five components:

- GRN (Giant Resonance Neutrons): neutrons generated in the core of the electromagnetic cascade by means of the giant-resonance production mechanism, with neutron energies below 20 MeV.
- HEN (High Energy Neutrons): neutrons with energies above 100 MeV, resulting from hadronic cascade initiated by high-energy photons above the photo-pion production threshold. This component is the most penetrating and dominates behind very thick shielding, but it manifests itself mostly by its byproduct, the lower-energy evaporation neutrons generated in outer layers of the shield.
- MID (Mid Energy Neutrons): neutrons with energies between those for GRN and HEN, including those generated by means of the pseudo-deuteron production mechanism.
- GamD (Direct Gammas): Photons escaping from the electromagnetic cascade core in a thick target, with energies in the 0.1 MeV to 20 MeV range. This range corresponds to the broad minimum in the mass attenuation coefficient for photons, called “Compton minimum”, of the shielding material. Note the original bremsstrahlung spectrum from electron interaction with material is a $1/k$ for thin targets or $1/k^2$ for thick targets (where k

is the photon energy and it can be as high as the electron beam energy). The fact that the spectrum outside shielding is populated with photons with energies near the “Compton minimum” region is the result of the spectrum hardening effect in shielding materials.

- GamI (Indirect Gammas): Photons and charged particles resulting from interactions of HEN and other neutrons in the shield and escaping from the shield material.

Yields and attenuation in the target material are calculated using the following parameters: atomic number Z and atomic mass A for target, photon mass attenuation factor μ , radiation length X_0 and Molière radius X_m . Parameters used to estimate attenuation in the shielding material are material density ρ , photon mass attenuation factor μ_s , and neutron mean-free-path factors λ_i , where $i = 1, 2, 3$ for the three neutron components (in g.cm^{-2}).

The total dose equivalent, consisting of photon dose equivalent H_p and neutron dose equivalent H_n , are calculated at a point of interest behind the shield, situated at an angle θ from the target. Assuming that the radiation field exhibits a “ $1/r^2$ ” variation (i.e., “point source”) with distance and attenuation is exponential, the model used in SHIELD11 is summed up in the two equations below for H_p and H_n :

$$H_p \left[\frac{\text{Sv.m}^2}{\text{h.kW}} \right] = 0.225 \times \left[\frac{\cos(\alpha - \theta)}{a + d} \right]^2 \times \left[\underbrace{\left(1.26 \times 10^6 E \times e^{-(t-0.01X_0)\mu} \times e^{-\theta^{0.6}} + 230 \times e^{-(r\mu-1.18)} \times e^{-\theta/72} \right)}_{\text{GamD}} \times e^{\frac{\mu_s d}{\cos(\alpha-\theta)}} + \underbrace{\frac{0.27}{(1-0.72 \cos \theta)^2} e^{\frac{d\rho}{\lambda_1 \cos(\alpha-\theta)}}}_{\text{GamI}} \right] \quad (4)$$

$$H_n \left[\frac{Sv.m^2}{h.kW} \right] = 0.225 \times \left[\frac{\cos(\alpha - \theta)}{a + d} \right]^2 \times \left[\underbrace{\frac{13.7 \times e^{-\frac{d\rho}{\lambda_1 \cos(\alpha - \theta)}}}{A^{0.65} (1 - 0.72 \cos \theta)^2}}_{HEN} + \underbrace{\frac{44.3 \times e^{-\frac{d\rho}{\lambda_2 \cos(\alpha - \theta)}}}{A^{0.37} (1 - 0.75 \cos \theta)}}_{MID} + \underbrace{4.94 Z^{0.66} e^{-\frac{d\rho}{\lambda_3 \cos(\alpha - \theta)}}}_{GRN} \right] \quad (5)$$

The source terms in SHIELD11 are not well suited for a thin target situation, such as when an electron beam hits a thin beam pipe wall under a glancing angle or electron beam is hitting a thin foil. For those thin-target cases, the results from Dinter and Tesch (1977), who measured experimentally the bremsstrahlung produced at various angles when a thin iron plate is struck at a glancing angle, can be used. Monte Carlo codes can also be used for the thin-target dose calculations. A variety of source terms for both thin and thick targets, including experimental data and Monte Carlo calculations, are also listed in the shielding compendium by Schopper et al. (Shopper et al.1990).

Shielding of Proton Accelerators

In this section aspects of production and shielding of the radiation fields at proton accelerators are discussed. Similar to electron accelerators, neutrons dominate the radiation fields outside the thick lateral shielding therefore particular emphasis is placed on the shielding against neutrons. To illustrate the basic concepts used in shielding, semi-empirical methods that are widely used for solution of practical shielding problems are discussed in this section.

For simple radiation protection calculations, Sullivan (1989) has developed a formula for the fluence of hadrons with $E_o > 40$ MeV that will be produced at one meter from a copper target struck by protons in the energy region $5 < E_o < 500$; E_o is in GeV and $\Phi(\theta)$ is in degree,

$$\Phi(\theta) = \frac{1}{2\left[\theta + \left(35/\sqrt{E_o}\right)\right]^2} \text{ (hadrons cm}^{-2}\text{)}(6)$$

At proton energies between about 0.05 and 5 GeV, this formula also approximately accounts for the distributions of neutrons per incident proton. This equation is plotted in Fig. 2, for "lateral" ($\theta=90^\circ$) and "forward" ($\theta=0^\circ$) directions. The dose equivalent result for $\theta=90^\circ$ is plotted in Fig. 3 by Tesch (1985). Above about 1 GeV, the dose equivalent is approximately proportional to E_o .

Neutron Shielding for Low Energy Incident Protons ($E_o < 15$ MeV)

Neutron shielding in this region is complex since this is the region of significant nuclear structure effects. In this energy region, there are many resonances associated with compound nucleus that can be excited and there are also many nuclear reaction channels leading to a large number of nuclear excited states up to 20 MeV in excitation energy which have a wide variety of nuclear structure quantum numbers and very narrow widths in energy. This effect complicates the shielding of neutrons in this energy range. A method, developed for reactor shielding, that is applicable to calculate shielding thicknesses in this energy domain is that of removal cross section theory (Patterson and Thomas 1973). To use the removal cross section method, there must be sufficient hydrogen in the shield. In this model the dose equivalent, H , as a function of shield thickness, t , is given by

$$H(t) = \Phi_o PG \exp(-\sum_r t), (7)$$

where ϕ_0 is the fluence before the shielding, P is the dose equivalent per fluence conversion factor, G is a "geometry factor", t (cm) is the thickness of the shield. For parallel beams, $G = 1$ while for an isotropic point source, $G = 1/r^2$. Σ_r is the macroscopic removal cross section;

$$\Sigma_r = \frac{0.602\sigma_r r\rho}{A} \text{ (cm}^{-1}\text{)}, (8)$$

where σ_r is the microscopic removal cross section in barns, r is the density (g cm^{-3}) and A is the mass number. For $A > 8$, and for neutrons of approximately 8 MeV;

$$\sigma_r \approx 0.21A^{-0.58} \text{ (barns)} (9)$$

Intermediate and High Energy Shielding-The Hadronic Cascade

At higher incident beam energies, hadronic cascade is initiated at proton accelerators when the beam interacts with targets, beam absorbers, and accelerator components to produce neutrons and other particles (Thomas and Stevenson 1988). Such cascades can also arise at electron accelerators since high energy secondary hadrons can also result from electromagnetic interactions.

The collision of a high energy nucleon with a nucleus produces a large number of particles; pions, kaons, and other nucleons as well as fragments of the struck nucleus. The neutrons may be classified as either evaporation neutrons or cascade neutrons. Evaporation neutrons originate as decays from excited states of residual nuclei and average a few MeV in energy. These neutrons tend to be isotropically distributed. Cascade neutrons are emitted by direct impact and their spectrum extends in energy up to the incident energy with diminishing probability following a spectrum roughly characterized as having an energy dependence proportional to $1/E$.

As the proton kinetic energy increases, other particles, notably pions and kaons play roles in the cascade when their production becomes energetically possible. They are absorbed with absorption lengths comparable in magnitude to those of protons. These particles also decay into muons. Because of their long ionization ranges and lack of nuclear interactions, muons provide a pathway for energy to escape the cascade.

In general, the neutrons $E_n > 150$ MeV are the principal drivers of the cascade because of the ionization energy loss for pions and for protons below 450 MeV where the ionization range becomes roughly equal to the interaction length. Furthermore, neutrons are produced in large quantities at large values of θ compared with the forward-peaked pions.

Intermediate and High Energy Shielding-Attenuation Length

An important feature of neutron shielding at higher energy (GeV energy region) accelerators is the fact that the attenuation length becomes an approximate constant at high energy. As the energy increases, the neutron inelastic cross sections increase rapidly until about 25 MeV where they generally level off and then fall rapidly with energy in the region $25 < E_n < 100$ MeV to a value which becomes independent of energy, aside from a slight, gradual increase at the very highest energies. This fact was discovered early in the history of accelerators by Lindenbaum (1961). The result is that high energy neutrons attenuate approximately exponentially with an attenuation length, λ_{atten} , that is rather insensitive to energy. Thus, in units of length,

$$\rho\lambda_{atten} = \frac{1}{N\sigma_{in}} \quad (cm) \quad (10)$$

where σ_{in} is the inelastic cross section and N is the number of absorber nuclei per unit volume. This cross section specifically does not include elastic scattering and so is always smaller than

the total cross section. Fig. 4 illustrates the neutron inelastic cross sections for several materials up to a kinetic energy of 1.4 GeV beyond which it is essentially constant.

Values of the high energy interaction lengths are available for many different materials and representative examples are provided by Schopper (1990) with extensive tabulations of the value of σ_{in} (mb) for a variety of particles, energies, and materials in the high energy region as functions of particle momenta up to 10 TeV/c.

The leveling off of the attenuation length for concrete as a function of particle energy is of special importance due to the widespread utilization of concrete shielding for hadrons. Fig. 5 gives the results for both neutrons and protons. An important feature of these results is the equivalence of the attenuation lengths for protons and neutrons at high energies.

Transverse Shielding of High-Energy Proton Accelerators

For both photons and neutrons, transmission through shield can be approximated by an exponential function. Ideally, the transmission factor, $T(z)$ of a shield of thickness z can be expressed as

$$T(z) = \exp[-z/\lambda] \quad (11)$$

where λ is the attenuation length. For a source point, for example neutrons produced in interaction of a proton beam on a beam intercepting device, the radiation level outside the shield may be written as

$$H(d, \theta) = r^{-2} H_{\theta} \exp[-d(\theta)/\lambda] \quad (12)$$

where r is the distance from the source, d is the shield thickness in the direction θ and λ is the effective removal mean free path and H_{θ} is the source term, that is the radiation level at zero shield in the direction H_{θ} at unit distance from the source.

This method, which is a point kernel method, can be used for calculating transverse shield of high-energy proton accelerators. The Moyer Model that was first developed by B. J. Moyer to solve particular shielding problems related to the Bevatron at the Lawrence Radiation Laboratory. The Moyer model is predominantly based on an exponential approximation with constants fitted to actual data spanning the range of proton beam energies from 7.4 to 800 GeV (Patterson 1973; Cossairt 2005; NCRP2003; Thomas and Stevenson 1988).

In Moyer model, the dose equivalent outside the shield at an angle of θ , from the beam-target interaction point (see Fig. 6.) is written as

$$H = \frac{H_o(E_p) f(-\beta t) \exp(-\zeta \csc \theta)}{(r \csc \theta)^2} \quad (13)$$

The shield materials are represented by the layers x_i and a is the inner radius of the tunnel. The dose point is at a radial thickness of d and is at a distance $r \csc \theta$ from the beam-target interaction point.

$$r = a + \sum_{i=1}^n x_i \quad (14)$$

The parameter ζ , which replaces the ratio d/λ in the argument of the exponential function, is introduced to take care of the n shielding components;

$$\zeta = \sum_{i=1}^n \frac{x_i}{\lambda_i} \quad (15)$$

Moyer model parameters have been determined empirically. (Stevenson et al. 1982; Thomas and Stevenson 1988) from global fits to data over a wide domain of energy that $f(\theta)$ is well described by

$$f(\theta) = \exp(-\beta\theta) \quad (16)$$

θ is in radians, β is in radians⁻¹, and, in fact, $\beta \approx 2.3 \text{ rad}^{-1}$ (for $En > 150 \text{ MeV}$) for proton kinetic energies above a few GeV.

The value of $H_o(E_p)\exp(-\beta\theta)$ is determined from the yield data and empirical measurements. $H_o(E_p)$ is best fit as a power law; $H_o(E_p) = kE_p^n$. From such results, per incident proton;

$$\begin{aligned} H_o(E_p) &= [(2.84 \pm 0.14) \times 10^{-13}] E_p^{(0.80 \pm 0.10)} \text{ (Sv m}^2\text{)} \\ &= 2.84 \times 10^{-8} E_p \text{ (mrem m}^2\text{)} = 2.8 \times 10^{-4} E_p^{0.8} \text{ (mrem cm}^2\text{)}. \end{aligned} \quad (17)$$

These results are derived for relatively "thick" targets (like accelerator magnets) in tunnel configurations. Schopper et al. (Sc90), based on Monte Carlo results gave values for "thin" targets of $k=2.0 \times 10^{-14}$ (Sv m²) and $n=0.5$ recommended values of λ for concrete and other materials as a function of mass number A are;

$$\text{Concrete: } 1170 \pm 20 \text{ kg m}^{-2} = 117 \text{ g cm}^{-2}$$

$$\text{Others: } 428A^{1/3} \text{ kg m}^{-2} = 42.8A^{1/3} \text{ g cm}^{-2}$$

Since it was first developed in early 1960s Moyer Model has been used in design of shielding against high energy neutrons in several accelerators. It is a simple and elegant model that can be readily used for shielding, or a test for results obtained by Monte Carlo methods. However, it is important to understand the limitation of the model. The source strength parameter was determined for small target to shield distance and normal to thick targets. Any large deviation of these conditions may result in wrong shield specifications. (Stevenson 1982)

Shielding Against Muons at Accelerators

Muons at proton accelerators arise from two principal mechanisms from pion and kaon decay and from direct production. Muons production becomes energetically possible at proton accelerators of energy above 150 MeV. However, for radiation protection, it will become a significant issue only when the primary beam energy is above 10-20 GeV for the longitudinal shield.

At electron accelerators, muons are generated by pair-production as well as pion and kaon decay. However, the fluences produced by direct photo-production is the dominant mechanism in electron accelerators (Nelson 1968; Nelson et al. 1974a; Nelson et al 1974b). Muon pair-production becomes possible at photon energies larger than > 211 MeV. Photo-muons are highly peaked in forward direction (angle < 10 mrad).

Muons are attenuated in the shield through ionization energy loss and multiple scattering. Radiative losses become important only in the TeV energies. Therefore, the muons are typically ranged out in the shield. For shielding of very high-energy muons (hundreds of GeV) only the use of earth as shield is practical. The energy-loss mechanism for muons is dominated by statistical fluctuations (straggling) at high energies and a significant number of muons have ranges much larger than the mean range.

Sullivan's approximation for muons is a method of estimating muon flux densities at proton accelerators based upon a semi-empirical fit to existing muon production data (Sullivan 1992). Sullivan gives an equation for the flux density of muons per meter of decay path as a function of shield thickness found along the proton beam axis (that is, on the straight-ahead maximum of the muons);

$$\Phi = 0.085 \frac{Eq}{\chi^2} \exp\left\{-\frac{\alpha t}{E}\right\} \quad (18)$$

where Φ is the fluence (muons m^{-2}) per interacting proton, E is the proton beam energy (GeV), χ is the distance of the dose point to the point of production of the pions and kaons (meters), q is the average path length (i.e., the decay path) of the pions and kaons in air, gases, or vacuum prior to their absorption by solids or liquids, and α is an effective average energy loss rate (GeV meter^{-1}) for the muons in a shield of thickness t (meters). For concrete, iron and lead, which

comprise the most commonly shield materials for muon shield, α is 9, 23 and 24 GeV m⁻¹ respectively. The full width at half maximum, FWHM, of the muon distribution at the boundary of such a shield is given by Sullivan;

$$FWHM = 4.6 \frac{\chi}{\sqrt{E\alpha t}} \text{ (meters)} \quad (19)$$

Attenuation by Ducts and Penetrations

All accelerators shields require openings to allow for personnel access, cable ventilations ducts water pipes, etc. Such penetrations could compromise the integrity of the shield and must be designed such that they do not undermine the overall efficiency of the shield. Various methods that are based on experimental data, albedo coefficient, empirical methods and Monte Carlo simulations exist.

Shield penetrations should not be placed such that there would be a line-of-sight to the primary beam. Additionally, the sum of shield wall thickness required between the source and the exit of the penetration should be the same as if the labyrinth were not present.

The existing data shows that incident particle energy or particle type does not affect the attenuation provided by a labyrinth viewing a source of beam loss other than the fact that the total yield of "source" neutrons depends on the incident energy and ion type. One can thus estimate the dose, dose equivalent, or neutron fluence at the exit of a labyrinth by using attenuation estimates in the legs multiplied by an estimate of the neutron fluence or dose equivalent found at the entrance, or mouth, of the penetration into the beam enclosure as show in Fig. 7.

For straight penetrations (first leg of a multi-legged access tunnel or shaft), and for the second, third and all the subsequent legs universal transmission curves are widely used for different source geometries (Goebel et al. 1972; Cossairt1995). The data are usually presented in units of d/\sqrt{A} where d is the distance from the source and A is the cross-sectional areas of the tunnel. The validity of scaling is for a height/width ratio that lies between 0.5 to 2.

Discussion of Shielding Materials

Attenuation of radiation intensities to the design levels can be achieved by a single material, or a particular combination of materials. Selection of shield materials and configuration could on factors other than their attenuation properties. To decide upon a final shield design, the following factors should also be considered (NCRP 2003):

- required thickness and weight of the material
- possibility of use as shielding against photons and neutrons
- uniformity, consistency and homogeneity
- cost, including cost of installation and maintenance
- shield design must be integrated with all other aspects of an accelerator facility
- possibility of induced radioactivity

Experience has shown that three materials concrete-earth and steel are the widely used as shield materials in high-energy accelerators. Cost considerations at large accelerators direct the usage of these particular materials. Other materials such as lead, polyethylene are used in special cases. In low energy electron accelerators, mainly medical and industrial accelerators of less than 10 MeV, lead is the shield of choice.

Earth

The main constituent of dry soil is SiO_2 making it an effective shield material for both

photons and neutrons. Depending on the soil type, water content and the degree of compaction, the earth density varies from 1.7 g cm^{-3} to as high as 2.25 g cm^{-3} . Earth may be easily put in place and is usually readily available, especially in large accelerators that are placed underground.

Concrete

Concrete is the material that is used widely as shielding materials in accelerators, due to its relative low cost, ease of case to different shapes, good structural properties and use as both photon and neutron shield. Concrete can be used either in the form of modular and moveable blocks that can be used as temporary shielding, or as reinforced concrete poured in place as structure that contains the accelerator. Portland concrete is a relatively standard material with the density in the range of $2.3\text{-}2.4 \text{ g cm}^{-3}$. Heavy materials can be added in the concrete aggregate, barites or iron ore, to increase its density and average Z , thus increasing its effective for photon shielding. The density of heavy concrete can exceed 4.5 g cm^{-3} , but this will come at a great increase in cost.

The water content of concrete, which may vary with time, and earth shield is of great importance in their efficiency for use as shield against neutrons. Residual radiation from ^{24}Na produced in concrete can be a major contributor to the ambient radiation levels after accelerator shut-down. Low-sodium aggregate are used to reduce thermal neutron induced radioactivation of concrete; alternatively, addition of boron compounds (boron frits) improves the thermal neutron absorption of concrete shield.

Iron

Iron or steel is widely used for photon shielding due to its relatively high density, low cost and good structural and thermal properties and ease of fabrication. The density of cast iron can be as

low as 7.0 g cm^{-3} ; steel density is typically around 7.9 g cm^{-3} . Steel, in conjunction with hydrogenous materials such as concrete, is used for shielding of high-energy neutrons (several tens of MeV), but is deficient for shielding low-energy neutrons. Steel contains no hydrogen, and its lowest inelastic energy level (i.e., in the dominant naturally-occurring iron isotope, ^{56}Fe) is 847 keV. Additionally, the 27.7 keV resonance and 73.9 keV resonance can result in large fluxes of soft neutrons outside iron shields. The effectiveness of the relative high energy of the lowest inelastic energy level in ^{56}Fe in greatly limiting the effectiveness of iron shielding for low energy neutrons has been discussed elsewhere (i.e., Elwyn and Cossairt 1986).

Polyethylene

Due to its large hydrogen content (~5% by weight) and its density of 0.92 g cm^{-3} polyethylene is used widely in shielding of D-T generators. Thermal neutron capture in polyethylene can lead to a build up of 2.2 MeV photons which can be mitigated by addition of a boron compound.

ACKNOWLEDGEMENTS

As a review article, this work is essentially a compilation of work done by others listed in references below, most prominently by Cossairt 2007, Destabler 1965, Nelson 2005, Thomas and Stevenson 1988, Shopper *et al* 1982, Swanson, 1979 and Vyelt and Liu 2001. This work was supported by Department of Energy Contract DE-AC-03-76SF00515.

References

- Cossairt JD. Radiation physics for personnel and environmental protection. Rev. 9B. Batavia, IL: Fermi National Accelerator Laboratory Report TM-1834; 2007. Available at: http://www-esh.fnal.gov/TM1834_PDF_Files/TM_1834_Revision_9B.pdf. Accessed 22 June 2007.
- Cossairt JD. Approximate technique for estimating labyrinth attenuation of accelerator-produced neutrons. Batavia, IL: Fermi National Accelerator Laboratory Fermilab Radiation Physics Note No. 118; October 1995.
- DeStaebler H. Similarity of shielding problems at electron and proton accelerators, Stanford, CA: Stanford Linear Accelerator Center Report SLAC Pub. 179; 1965.
- Dinter H., Tesch K. Dose and shielding parameters of electron-photon stray radiation from a high-energy electron beam, Nucl Instr & Meth. 143, 349-355; 1977.
- Elwyn AJ, Cossairt JD. A study of neutron leakage through an Fe shield at an accelerator. Health Phys 51:723-735; 1986.
- Fasso A, Ferrari A, Ranft J, Sala PR. FLUKA, a multi-particle transport code. Geneva, Switzerland: European Center for Nuclear Research Report CERN-2005-10, INFN/TC_05/11, SLAC-R-773; 2005.
- Goebel K, Stevenson GR, Routti RJ, and Vogt HG. Evaluating dose rates due to neutron leakage through the access tunnels of the SPS. European Center for Nuclear Research Report CERN LABII-RA/Note/75-10; 1975.
- Ipe N, Liu JC. Shielding and radiation protection at the SSRL 3 GeV injector. In: New horizons in radiation protection and shielding. Proceedings of American Nuclear Society Topical

Meeting; Pasco, Washington; 1992.

Iwase H, Niita K, and Nakamura T. Development of general-purpose particle and heavy ion transport Monte Carlo code. *Journal of Nuclear Science and Technology* 39: 1142-1151; 2002.

Lindenbaum SJ. Shielding of high energy accelerators. *Ann Rev Nucl Sci* 11:213-258;1961.

Liu JC, Mao ZS, Nelson WR, Seeman J, Schultz D, Bong P, Gray P, Radiation safety system of the B factory at the Stanford Linear Accelerator Center. *Health Phys.*77:588-594,1999.

Liu JC, Bull JS, Drozdoff J, May R, Vylet V. Radiation safety systems for accelerator facilities *Rad Pro.Dos.*96:429-440; 2001.

Liu JC, Vylet V, Walker LS. Engineered and Administrative Safety Systems for the Control of Prompt Radiation Hazards at Accelerator Facilities, this compendium; 2007.

McKinney GW, et al., MCNPX 2.6.X features (2006-2007). Los Alamos National Laboratory Report LA-UR-07-2053, M&C/SNA 2007.

Mokhov NV. The MARS code system user's guide. Version 13. Batavia IL: Fermi National Accelerator Laboratory Report FN-628; 1995.

National Council on Radiation Protection and Measurements. Radiation protection for particle accelerator facilities. Bethesda, MD: NCRP Report No. 144; 2003.

Nelson WR, Jenkins TM. The SHIELD11 computer code. Stanford, CA: Stanford Linear Accelerator Center Report SLAC-R-737, UC-414; 2005.

Nelson WR, Rokni SH. SHIELD11: A line source application of SHIELD11. Stanford, CA: Stanford Linear Accelerator Center Report SLAC-TN-06-002; 27 April 2006.

Nelson WR. The shielding of muons around high-energy electron accelerators: Theory and

- measurement. Nucl Instr & Meth. 66: 293-303; 1968.
- Nelson WR, Hirayama H, Rogers DWO. The EGS4 code system. Stanford CA: Stanford Linear Accelerator Center. SLAC Report No. SLAC 235; 1985.
- Nelson WR, Kase KR. Muon shielding around high-energy electron accelerators, part I, theory, Nucl Instr and Meth 120:401-411; 1974
- Nelson WR, Kase KR, Stevenson GR. Muon shielding around high-energy electron accelerators, Part II, Experimental investigation. Nucl Instr and Meth 120:413-429;1974.
- Patterson HW, Thomas R H. Accelerator health physics. New York, NY: Academic Press; 1973.
- Rokni SH. et al., Benson EC, Burke DL, Jenkins T, Helson G, Nelson WR, Smith HE, Tenenbaum, PT, Walz, DR, Vylet, Radiation protection systems for the final focus test beam at SLAC. Health Phys 71:786-794; 1996.
- Schopper H. Fassò A, Goebel K, Höfert M, Ranft J, Stevenson G. Landolt-Börnstein numerical data and functional relationships in science and technology new series; Group I: nuclear and particle physics Volume II: Shielding against high energy radiation. O.Madelung, Ed. Heidelberg and Berlin: Springer-Verlag; 1990.
- Stevenson G , Kuei-Lin L, Thomas RH. Determination of transverse shielding for proton accelerators using the Moyer model. Health Phys 43:13-29; 1982.
- Sullivan A H. The intensity distribution of secondary particles produced in high energy proton interactions. Rad Prot Dos 27:189-192, 1989.
- Sullivan A H. A guide to radiation and radioactivity levels near high energy particle accelerators. Ashford, Kent, United Kingdom: Nuclear Technology Publishing;1992.
- Swanson W P. Radiological safety aspects of the operation of electron linear accelerators

Vienna, Austria: International Atomic Energy Agency IAEA Technical Report No. 188; 1979.

Tesch K. The attenuation of the neutron dose equivalent in a labyrinth through an accelerator shield, Part Accel 12:169-175,1982.

Tesch K. A simple estimation of lateral shielding for proton accelerators in the energy range from 50 to 1000 MeV, Rad Prot Dos 1, 165-172, 1985.

Thomas RH, Thomas SV. Variation and regression analysis of Moyer model parameter data, Health Phys 46:954-957; 1984.

Thomas RH, Stevenson GR. Radiological safety aspects of the operation of proton accelerators, Vienna Austria: International Atomic Energy Agency IAEA Technical Report No. 283;1988.

Vylet V. Prompt radiation fields at accelerators; this compendium; 2007.

Vylet V, Liu JC. Radiation protection at high-energy electron accelerators, Rad Prot Dos 96:333-343; 2001.

List of Figure Captions

Fig. 1: Geometry representation used in the SHIELD11 code: Photon and neutron dose equivalent is calculated at a point behind a primary slab shield. Additional “local” shielding of different material, situated between the target and the point of interest, can be taken into account. See text for the meaning parameters describing properties of target and shielding. HEN refers to neutrons with energies above 100 MeV, MID neutrons have energies between 100 MeV to 20 MeV, GRN neutrons have energies below 20 MeV.

See text for the meaning parameters describing properties of target and shielding.

Fig. 2. Plot of Eq. for two different values of θ . The proton is interacting in a copper target [(Sullivan 89).]

Fig. 3. Dose equivalent per proton due to neutrons at $\theta=90^\circ$ having energies higher than 8 MeV at a distance of 1 meter from a copper target. The curve is an interpolation between the normalized experimental measurements denoted by the open symbols. [Adapted from Tesch 1985).]

Fig. 4. Inelastic neutron cross sections as a function of energy in the range 1 to 1000 MeV. [Adapted from (Lindenbaum 1961)].

Fig. 5. The variation of the attenuation length λ for monoenergetic neutrons and protons in concrete shielding as a function of neutron energy. The high energy limit is 117 g cm^{-2} . (Adapted from Stevenson 1982)

Fig. 6. Geometry for the empirical Moyer Model. A beam of protons impinges on the target of length L . The shield materials are represented by the layers x_i ; a is the inner radius of the tunnel. The dose point is at a radial thickness of d and is at a distance $r \csc \theta$ from the beam-target interaction point.

Fig. 7. Schematic plan view of a typical personnel access labyrinth of three “legs” at a large accelerator facility that defines the coordinate system and terminology associated with labyrinth calculations. The (*) denotes the location of a loss of beam at a point adjacent to the “mouth” of the labyrinth. The lengths of legs after the first are measured between centers of turns.

Fig. 8. Universal transmission curves for the first leg of a labyrinth as a function of normalized distance, δ_1 from the mouth. The curve for a plane source is also suitable to use with an off-axis point source. Adapted from (Goebel 1975 and Cossairt 1995).

Fig. 9. Universal transmission curve for the second and subsequent legs of labyrinths as a function of normalized distance from the center of the previous turn, δ_i . [Adapted from (Goebel 1975) and (Cossairt 1995).]

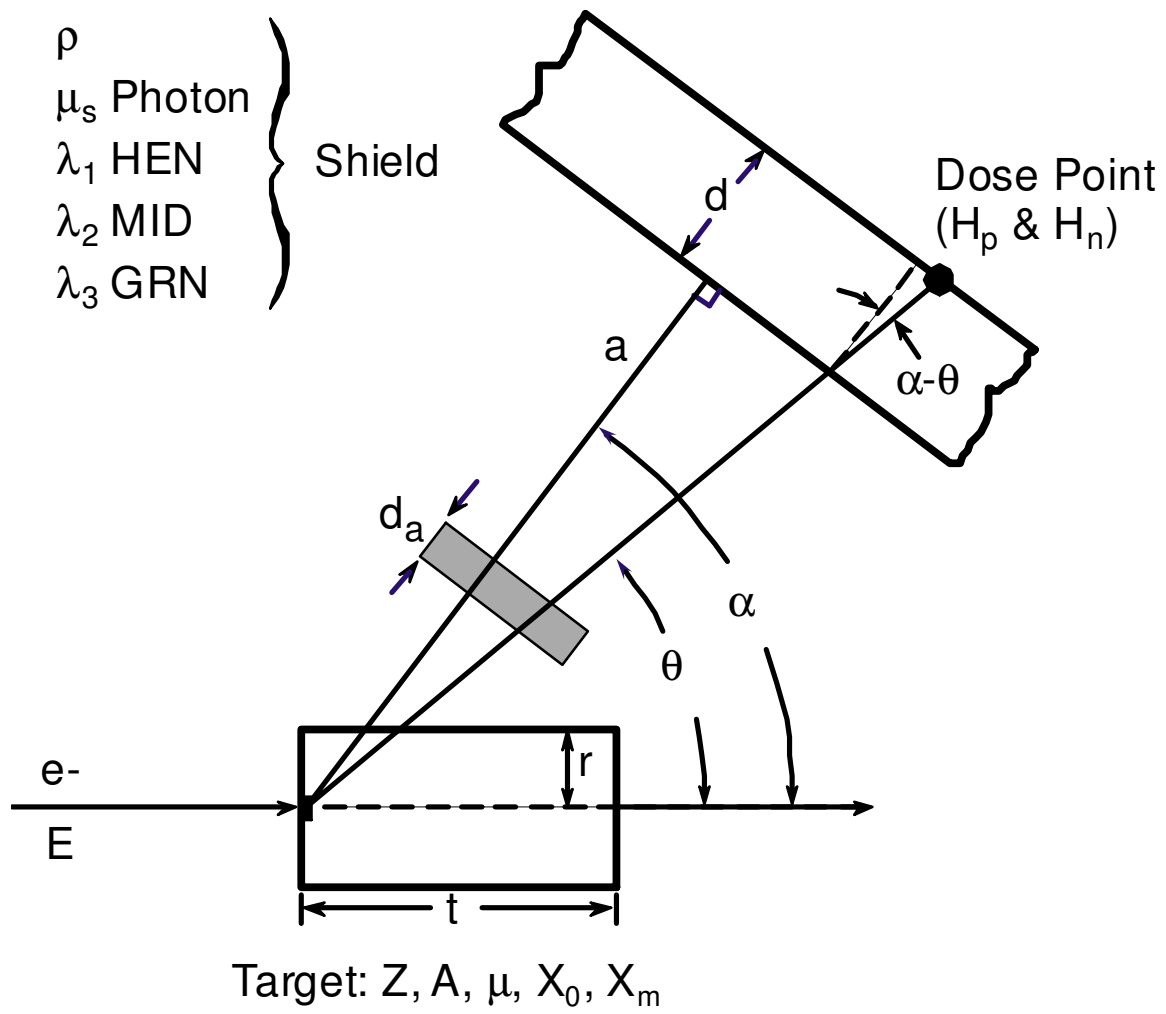


Fig. 1

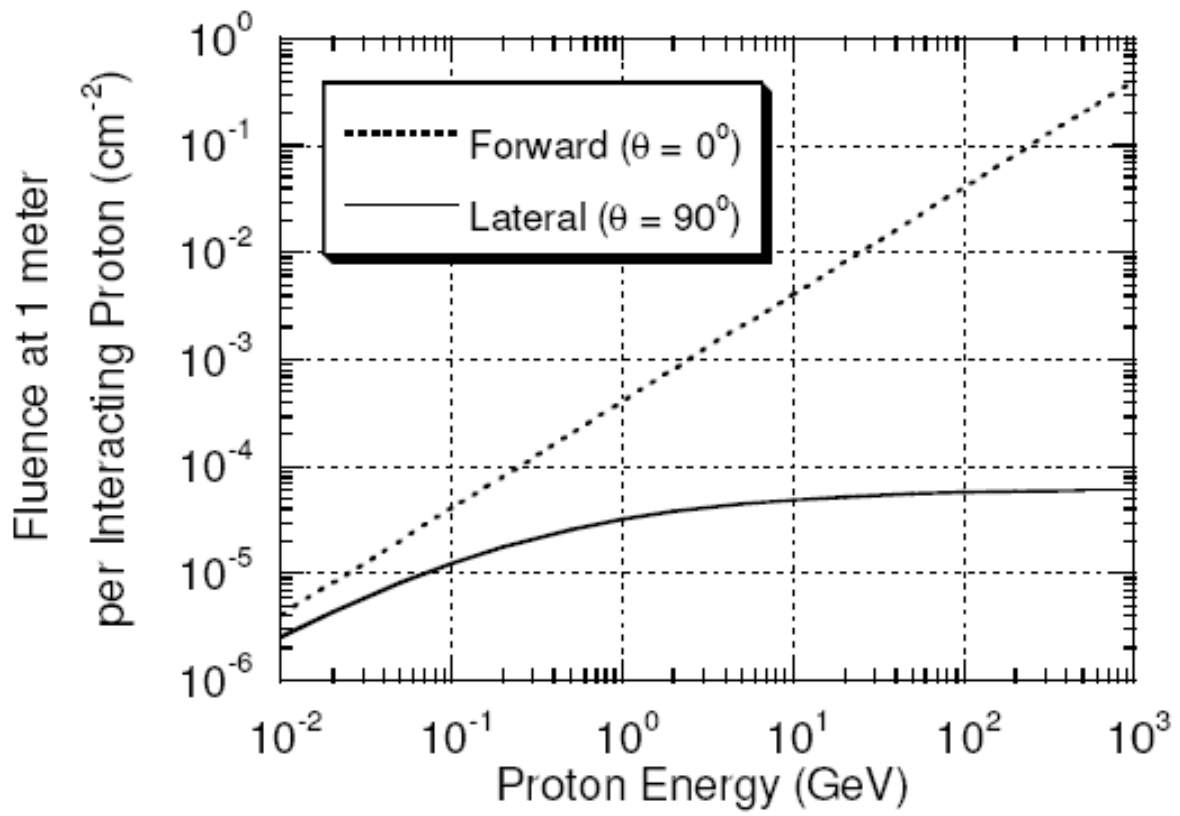


Fig. 2.

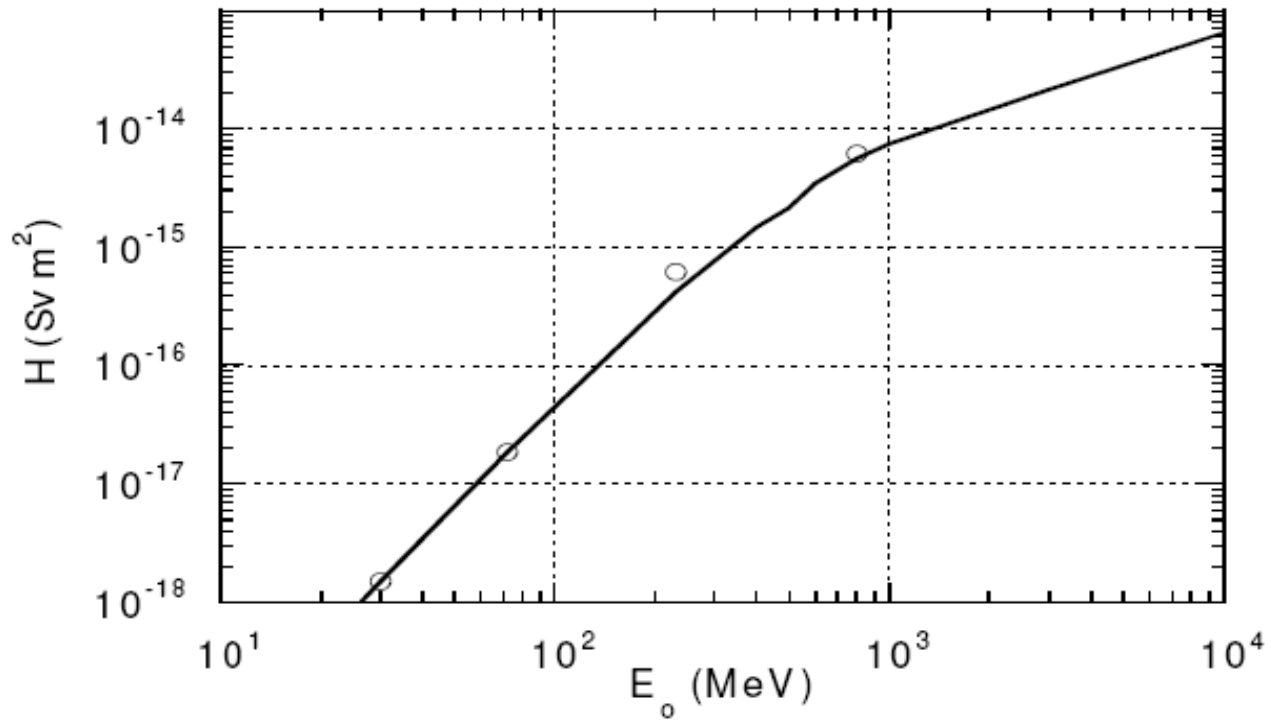


Fig. 3.

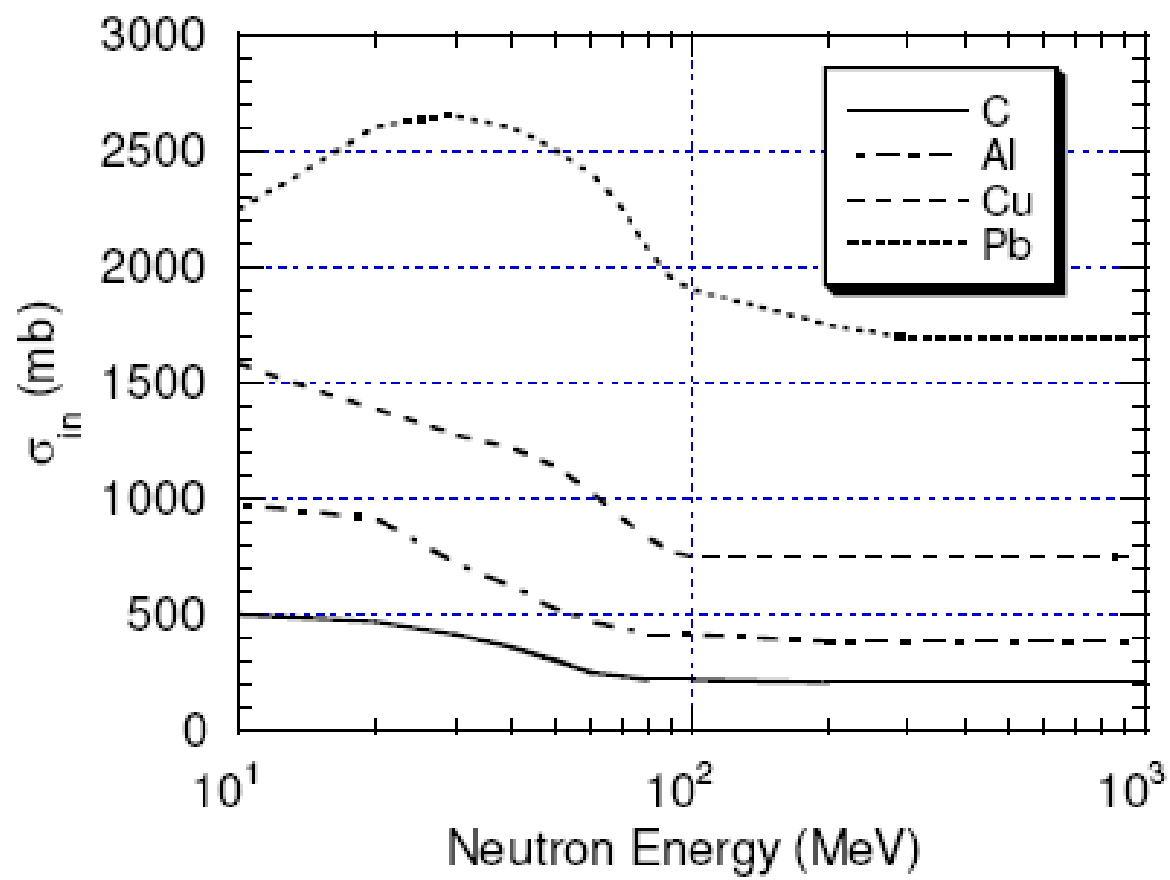


Fig. 4

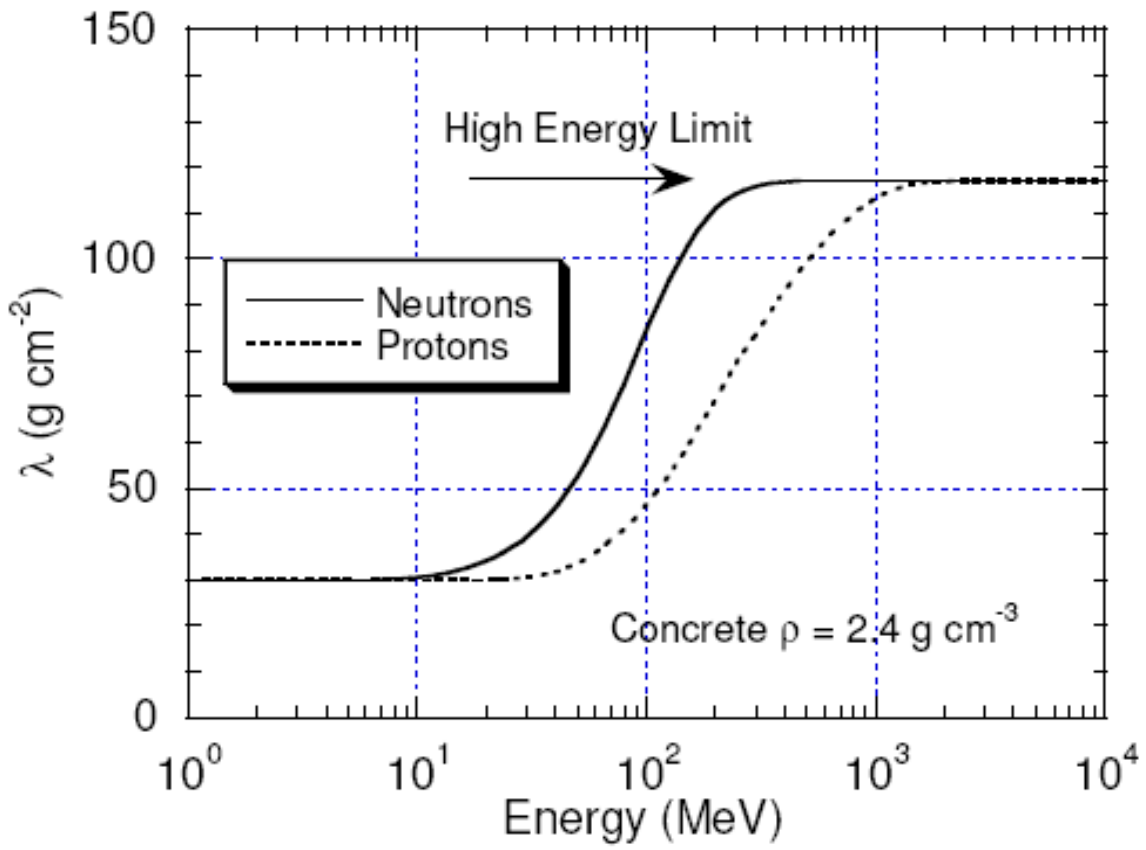


Fig. 5.

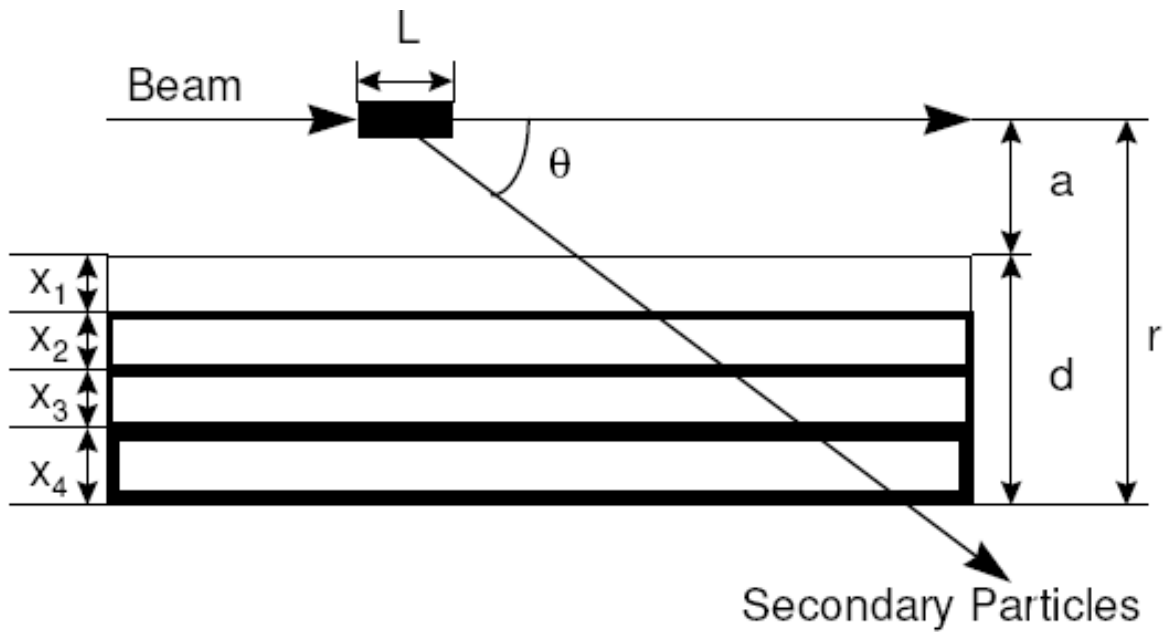


Fig. 6.

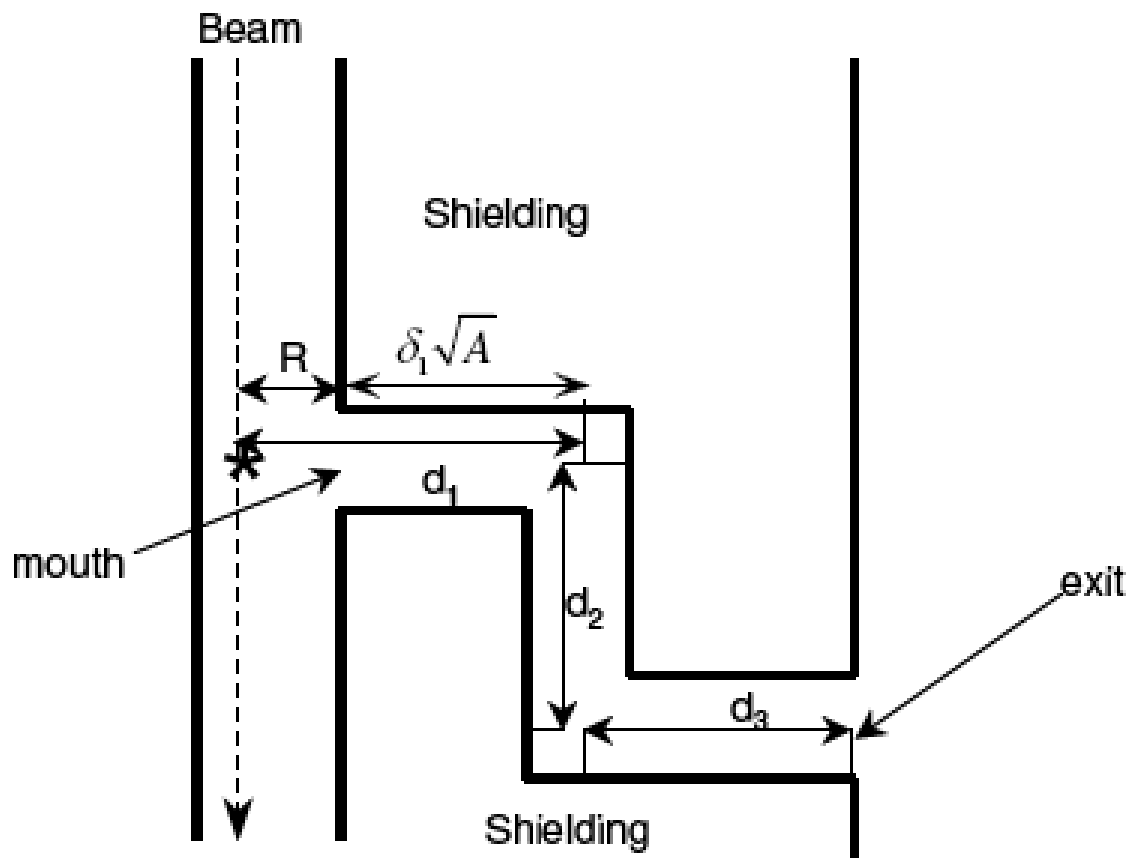


Fig. 7.

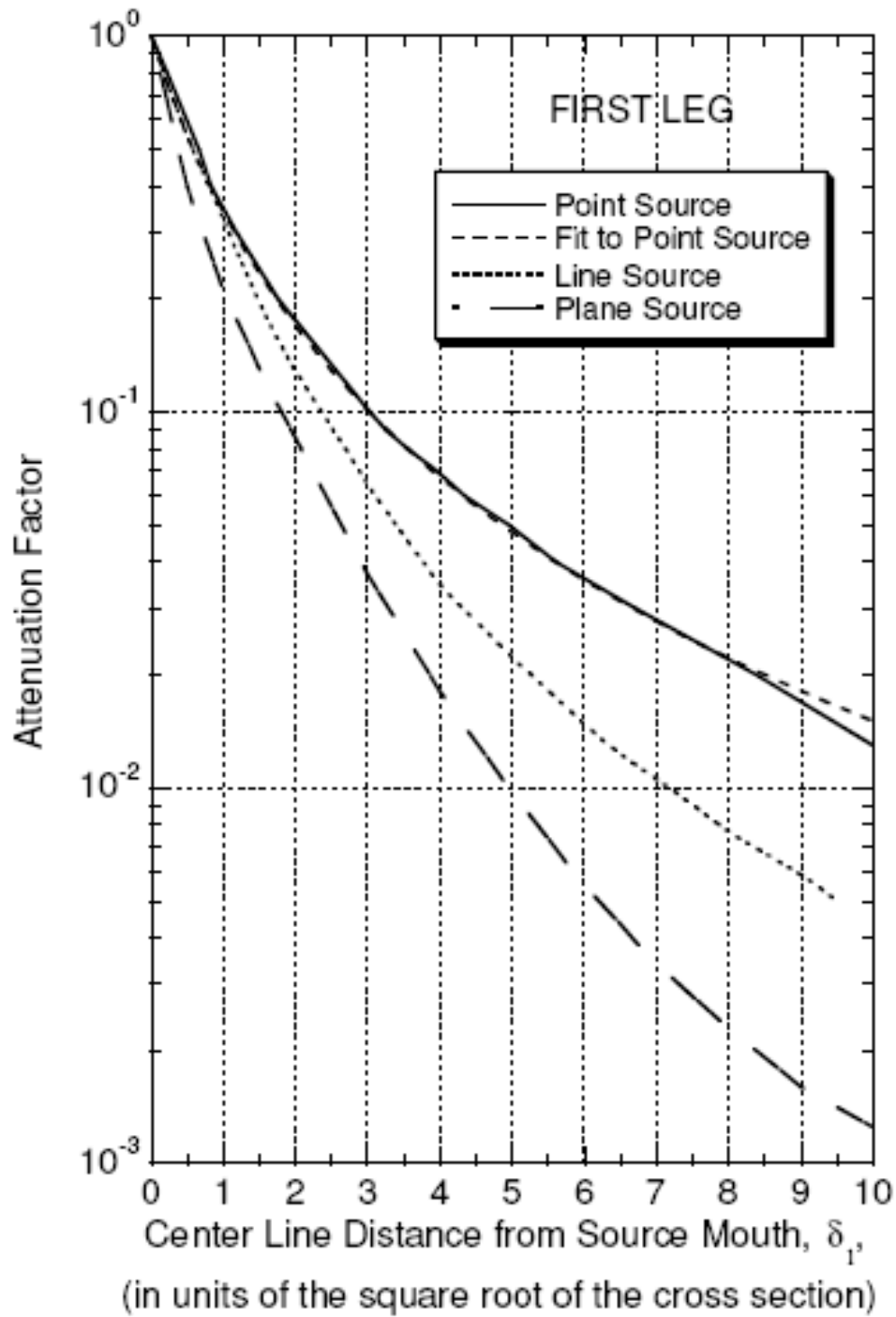


Fig. 8.

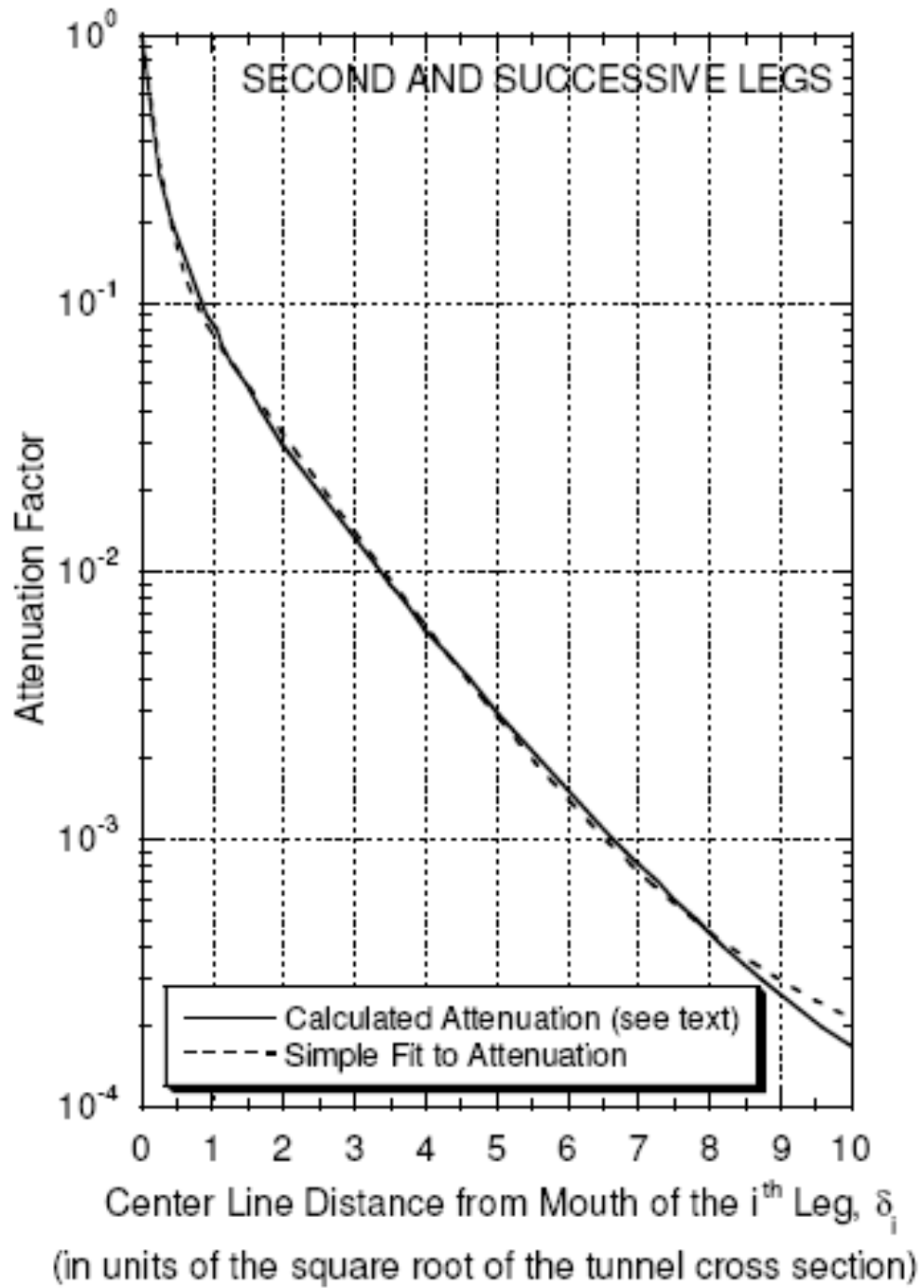


Fig. 9.